Microchim Acta (2011) 174:97–105
DOI 10.1007/s00604-011-0585-4

ORIGINAL PAPER

Biocompatible and label-free amperometric immunosensor for hepatitis B surface antigen using a sensing film composed of poly(allylamine)-branched ferrocene and gold nanoparticles

Jian-Ding Qiu · He Huang · Ru-Ping Liang

Received: 11 December 2010 / Accepted: 4 March 2011 / Published online: 12 April 2011

Abstract An amperometric immunosensor has been developed for sensitive determination of hepatitis B surface antigen as a model protein. A glassy carbon electrode was modified with an assembly of positively charged poly(allylamine)-branched ferrocene (PAA-Fc) and negatively charged gold nanoparticles (Au NPs). The formation of PAA-Fc effectively avoids the leakage of Fc, retains its electrochemical activity, and enhances the conductivity of the composite. The adsorption of Au NPs onto the PAA-Fc matrix provides sites for the immobilization of the antigen and a favorable microenvironment to maintain its activity. The morphologies and electrochemistry of the sensing film were investigated via scanning electron microscopy, electrochemical impedance spectroscopy, and cyclic voltammetry. Factors influencing the performance of the immunosensor were studied in detail. The concentration of the antigen can be quantitated (by measuring the decrease of the amperometric response resulting from the specific binding between antigen and antibody) in the range between 0.1 and 150 ng mL^{-1}, with a detection limit of 40 pg mL^{-1} (S/N = 3). The method is economical, efficient, and potentially attractive for clinical immunoassays.

Keywords Amperometric immunosensor · Poly(allylamine) · Ferrocene · Gold nanoparticles · Hepatitis B surface antigen

Introduction

Hepatitis B virus (HBV) infection occurs worldwide and is one of the major causes of acute and chronic viral hepatitis. In the United States, approximately 300,000 new cases of HBV infection are reported each year, and it is estimated that more than 300 million people worldwide are chronic carriers of the virus [1]. Patients infected with the virus can develop life-threatening cirrhosis and liver cancer, undergoing great physical pain or mental anguish. General research demonstrated that Hepatitis B surface antigen (HBsAg) is a major index of hepatitis B viruses [2]. Recently, many efforts have been made to develop various immunoassay methods including radioimmunoassay [3], enzyme-linked immunosorbent assay (ELISA) [4], fluoroimmunoassay [5], and chemiluminescent immunoassay [6] for rapid and sensitive detection of HBsAg. Although these detection techniques provide advantages (e.g., sensitivity, precision and selectivity), they often suffer from some limitations because they present radiation hazards, take tedious assay time, have high cost, and require qualified personnel and sophisticated instrumentation [7]. Thus, a simple, sensitive and convenient method for the determination of HBsAg in human serum is desirable.

Electrochemical immunoassays which are based on specificity of antigen–antibody interactions with electrochemical transduction for analytical purpose [8], have been considered as excellent candidates for the rapid and inexpensive diagnosis of genetic diseases and for the

Electronic supplementary material The online version of this article (doi:10.1007/s00604-011-0585-4) contains supplementary material, which is available to authorized users.

J.-D. Qiu (✉) · H. Huang · R.-P. Liang
Department of Chemistry and Institute for Advanced Study, Nanchang University,
Nanchang 330031, People's Republic of China
e-mail: jdqiu@ncu.edu.cn

detection of pathogenic biological species of clinical interest. Among several kinds of immunosensors, amperometric immunosensor have attracted more interests recently due to their advantages such as simple pretreatment procedure, precise and sensitive current measurements, and low-cost and miniaturizable instrumentation [9, 10]. Since both antigen and antibody are electrochemically inert, most amperometric immunosensors, unfortunately, require labeling of either immunocomponent [11], which processes highly qualified personnel, tedious assay time, or sophisticated instrumentation. As a result, much attention has been focused on the reagentless and label-free electrochemical immunosensors [12, 13]. However, the addition of mediator such as ferrocene and its derivatives, dyes, hydroquinone, hexacyanoferrates etc. in the analyte solution [14–18] would cause electrode contamination, reagent-consuming and operation inconvenience. To solve these problems, it should be preferable to immobilize mediators on electrode surfaces to construct amperometric immunosensors [19–21]. Yang and co-workers synthesized water-soluble electroactive polymers via incorporation ferrocene moieties onto dendrimer polymer and used to construct a highly sensitive electrochemical immunosensor for detection of IgG, covalently bound Fc with dendrimer polymer can not only effectively prevent leakage of ferrocene from the electrode surface during the detection process, but also endow polymer with conductive and advanced properties [22]. The conjugation of mediator ferrocene to inert protein bovine serum albumin has been reported by Tripathi et al. [23], which could inhibit the leakage of mediator away from electrode surface effectively. Our group synthesized water-soluble electroactive polymers via incorporation ferrocene moieties onto chitosan to prevent the leakage of mediator and facilitated electron transfer between the enzyme and electrode [24]. In this work, poly(allylamine) (PAA), a weak polyelectrolyte with well water-solubility and biocompatibility which carries positive charges at suitable pH [25], was chosen to covalent conjugate with ferrocene (Fc) group to form a novel redox-active hybrid material. This strategy can not only effectively prevent leakage of Fc from the matrix and remain the biocompatibility of PAA, but also combine redox activity and biocompatibility to the novel formed composite [26, 27]. In addition, the abundant amino groups in PAA backbone could offer great active sites for further Au NPs assembling [28], and thus, the Au NPs modified electrodes with very large surface area, are simple to fabricate and functionalize, retain metallic conductivity, and lend themselves to facile biomolecule attachment [29–31].

In this paper, we report on the design of a novel architecture to fabricate label-free HBsAg immunosensor by combining the biocompatibility and redox electrochemistry of PAA-Fc and excellent adsorption of Au NPs to HBsAb. A stable PAA-Fc composite film with redox activity, abundant amino groups and good biocompatibility was first formed on the electrode surface. Subsequently, Au NPs were adsorbed onto the PAA-Fc film surface through the well-developed interaction between Au NPs and amino groups of PAA, which provided reactive sites for further antibody immobilization. The results showed that this immobilization technique was effective in preventing the leakage of both mediator and antibodies. Compared with conventional immunoassay methods, the developed immunosensor is simple, economical and efficient towards the quantification of HBsAg, showing a great potential in clinical applications.

Experimental

Chemicals and reagents

Poly(allylamine hydrochloride) (MW: ~56, 000), ferrocenecarboxaldehyde (FcCHO, 98%), bovine serum albumin (BSA) and hydrogen tetrachloroaurate ($HAuCl_4 \cdot 4H_2O$) were purchased from Sigma-Aldrich (St. Louis, USA, www.sigmaaldrich.com). Hepatitis B surface antibody (HBsAb) and Hepatitis B surface antigen (HBsAg) were purchased from Bosai Chemical Reagent Co. (Zhengzhou, China, www.chinabiocell.com). All other chemicals were of analytical grade and used as received without further purification. 0.1 M acetate buffer solution (pH 5.5) was used as supporting electrolyte. All the solutions were prepared using doubly distilled water.

Apparatus and measurements

The size of the prepared monodispersed Au nanoparticles was determined from transmission electron microscopy (TEM, JEM-2010, Japan, www.jeol.com). Scanning electron microscopy (SEM) images were obtained with a Quanta 200 scanning electron microscope (FEI, USA, www.fei.com). Fourier transform infrared spectra (FTIR) were recorded on a Nicolet 5700 FTIR spectrometer (Nicolet, USA, www.thermofisher.com). All electrochemical experiments were carried out on an Autolab PGSTAT30 potentiostat/galvanostat (Eco Chemie, The Netherlands, www.labrecyclers.com). A conventional three-electrode system was used, the modified electrode as the working electrode, a platinum wire as the counter electrode, and Ag/AgCl (saturated KCl) as the reference electrode. The AC impedance experiments were performed in 0.1 M pH 5.5 acetate buffer solution containing 2.5 mM $K_3[Fe(CN)_6]$/$K_4[Fe(CN)_6]$ (1:1) and 0.1 M KCl by applying an alternating current voltage with 5 mV amplitude in a frequency range of 10^{-2}–10^5 Hz.

Preparation of Fc-branched PAA derivatives

PAA-Fc was synthesized according to the literature [32]. Briefly, PAA (40.0 mg) was dissolved in anhydrous methanolic solution (30 mL) containing 0.26 mL triethylamine. FcCHO (8 mg) was dissolved in methanol (5 mL) and then added into the above PAA solution. After the mixture was stirred at room temperature for 1 h, $NaBH_4$ (5.7 mg) was carefully added at 0 °C and the reaction mixture was stirred for another 1.5 h. Finally the mixture was dried in vacuo at 35 °C and the residue was extracted with distilled water. The aqueous solution was further purified by membrane dialysis against water.

Preparation of Au NPs

Au NPs with an average diameter of 12 nm were synthesized via reduction of $HAuCl_4{\cdot}4H_2O$ by trisodium citrate and tannic acid [33, 34]. The ratio of tannic acid to trisodium citrate determines the size and distribution of synthesized Au NPs. Two initial aqueous solutions (a) 1 mL of 2 wt.% $HAuCl_4{\cdot}4H_2O$ solution, which was diluted to 80 mL, and (b) a mixture of 8 mL of 1 wt.% trisodium citrate and 0.2 mL of 1% tannic acid, which was diluted to 20 mL, were heated to 60 °C on a hot plate. Then, solution (b) was rapidly added to solution (a) under rigorous stirring for 35 min to give Au NPs solution. The concentration of as-synthesized Au NPs was determined to be 0.12 mg mL^{-1} on the basis of the concentration of $HAuCl_4{\cdot}4H_2O$ before reaction, assuming a 100% reduction yield of the $[AuCl_4]$ ions [35].

Preparation of the immunosensor

Glassy carbon electrode (GCE, 3 mm diameter, CH Instruments, Inc.) was wet polished down to mirror-like with 1.0, 0.3 and 0.05 mm alumina slurry, respectively, and rinsed thoroughly with doubly distilled water between each polishing step. The electrode was then successively sonicated in 1:1 nitric acid, acetone and doubly distilled water, and then allowed to dry at room temperature. After dropping 5 μL PAA-Fc solution on a cleaned electrode surface and then drying slowly in air at room temperature, the PAA-Fc modified electrode was immersed in the Au NPs solution for 12 h to form PAA-Fc/Au NPs nanocomposite. After washing with water, the electrode was dipped into a HBsAb (200 ng mL^{-1}) solution overnight at 4 °C to yield a sensing interface. Then unbounded antibodies were washed away with phosphate buffered saline (PBS). At last the PAA-Fc/Au NPs/HBsAb modified electrode was incubated in a solution of 0.25% BSA for 1 h at 37 °C to block possible remaining active sites of the nano-Au monolayer and avoid the non-specific adsorption in the further process. After the modified electrode was washed carefully with PBS three times, an immunosensor was fabricated and stored at 4 °C when not in use. The schematic illustration of the stepwise preparation of the immunosensor was shown in Scheme 1.

Immunoassay procedure for detection of HBsAg

The prepared immunosensor was incubated in 0.5 mL incubation solution containing various concentrations of

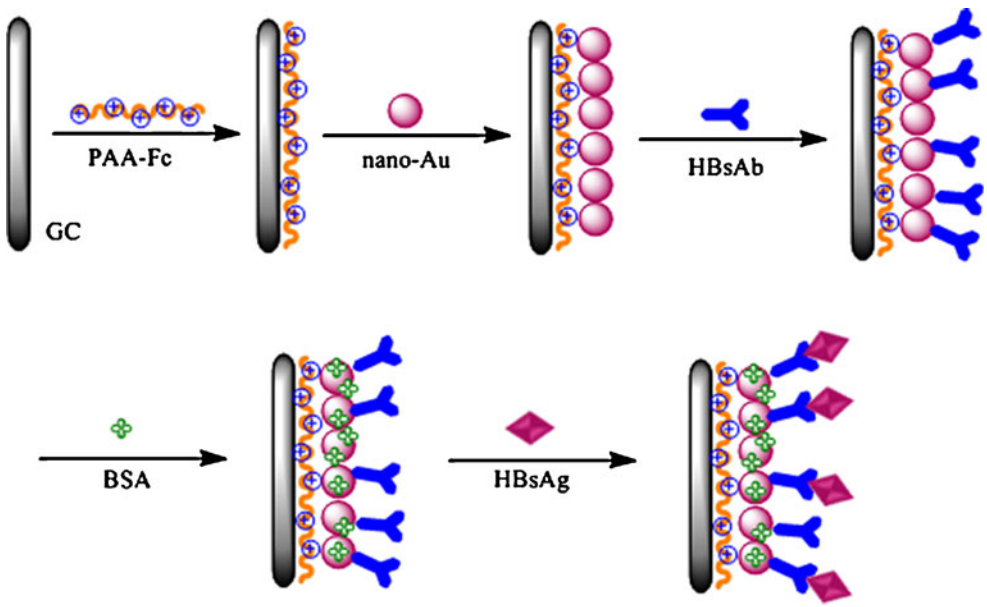

Scheme 1 Schematic diagram of the immunoassay procedure

HBsAg at 35 °C for 10 min. After washing carefully with pH 5.5 acetate buffer solution to remove the non-chemisorbed HBsAg, differential pulse voltammetric (DPV) responses of the immunosensor were recorded in 0.1 M pH 5.5 acetate buffer solution containing 0.1 M $KClO_4$. After the antigen–antibody reaction, the response current of redox probe Fc decreased due to the formation of immunocomplex, which was directly proportional to the concentration of antigen. According to the linear relationship, the detection of HBsAg in the sample solution can be assessed quantitatively.

Results and discussion

FTIR characterization of PAA-Fc

The aldehyde group of FcCHO can easily react with the amino group of PAA through formation of a Schiff base and subsequent reduction by $NaBH_4$. To realize the binding mechanism, the formation of PAA-Fc was confirmed by FTIR spectra (Fig. 1). The spectrum of FcCHO (Fig. 1a) shows an adsorption band centered at 1,680 cm^{-1} due to the free aldehyde groups vibration. The spectrum for PAA (Fig. 1b) shows two bands located at around 1,606 and 1,508 cm^{-1} which can be assigned to the amino I and amino II functional groups of the native PAA, respectively [36]. After FcCHO reacted with PAA, the spectrum of the resultant product (Fig. 1c) shows that the characteristic peak of FcCHO at 1,680 cm^{-1} (ν, C = O) disappeared and new absorption bands at about 480 cm^{-1}(δ, Fe-Cp) and 814 cm^{-1} (δ, C–H (Cp)) appeared, which indicated the successful formation of PAA-Fc composite. In addition, the absorption bands for amide I and amide II in PAA still exist, suggesting that there are free amino groups in PAA remaining and the native structure of PAA is not changed. These free amino groups offer sites for the further assembly of Au NPs.

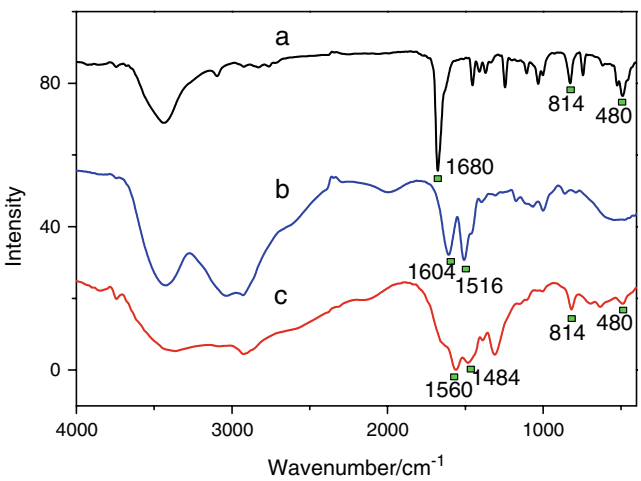

Fig. 1 FTIR spectra of **a** FcCHO, **b** PAA, and **c** PAA-Fc

Morphologies of different membranes

PAA is a weak polybase with many ionizable $–NH_2$ groups in its backbone [37, 38]. As a high-molecular weight polymer, PAA is positively charged at pH 5.5, whereas Au NPs are negatively charged. Therefore Au NPs can be easily self-assembled onto the side chain of the oppositely charged PAA due to the well-developed interaction between Au NPs and amino groups [39]. SEM was applied to character the morphology of the PAA-Fc, PAA-Fc/Au NPs, and PAA-Fc/Au NPs/HBsAb films. As can be seen from Fig. 2a, the SEM image of the PAA-Fc membrane displays an extreme smooth and homogenous structure. After absorption of Au NPs, many pearl-like particles distributed uniformly in the PAA-Fc matrix (Fig. 2b), and the formed PAA-Fc/Au NPs film with three-dimension structure provided a microenvironment and lots of binding centers for efficient alignment of biomolecules. When HBsAb was immobilized onto this PAA-Fc/Au NPs film, plentiful bright clusters appeared in the SEM image (Fig. 2c). These big clusters should be the adsorbed proteins, which increased the surface roughness. This suggests that the HBsAb was successfully immobilized on the surface of PAA-Fc/Au NPs film.

Electrochemical characteristics of the modified electrodes

Cyclic voltammetry (CV) is an effective and convenient method for probing the feature of the modified electrode surface. Figure 3 shows CVs of different modified electrodes in the potential range of 0.2–0.65 V in a pH 5.5 acetate buffer solution containing 0.1 M KCl at a scan rate of 50 mV s^{-1}. No redox peak was observed at both bare GCE and PAA/GCE (Fig. 3a and b), whereas the redox hybrid material PAA-Fc modified electrode shows a stable and well-defined redox peaks at 428 and 398 mV (ΔEp = 30 mV, $ipc/ipa \approx 1$) (Fig. 3c), indicating that Fc was covalently bounded in PAA chain. Deposition of Au NPs increased the conductivity of the PAA-Fc film, resulting in the increase of the anodic peak and cathodic peak currents (Fig. 3d) as the Au NPs acted as a conducting wire or an electron communication relay, which increased the electron-transfer efficiency [24, 40]. When the PAA-Fc/Au NPs modified electrode was incubated with HBsAb, the redox peak currents decreased and the peak-to-peak separation increased significantly (Fig. 3e), which indicated antibody has been successfully immobilized on the electrode surface on one hand, and on the other hand, the immobilized protein acted as insulator blocking the electron communication of the

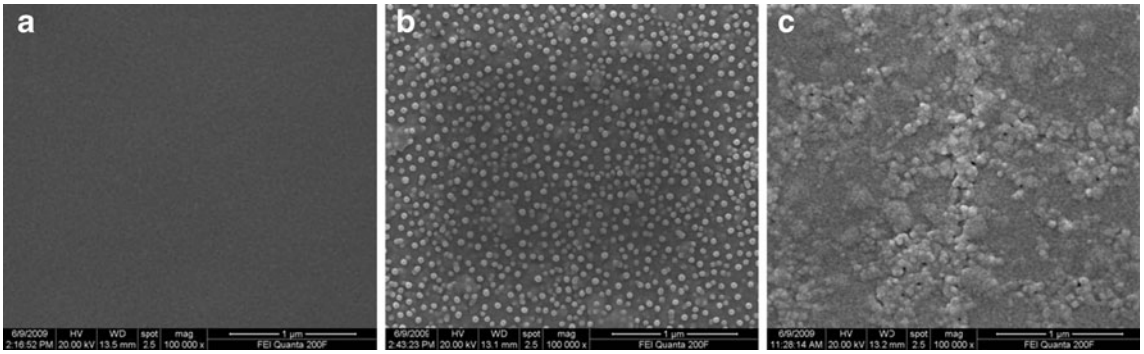

Fig. 2 SEM images of **a** PAA-Fc, **b** PAA-Fc/Au NPs, and **c** PAA-Fc/Au NPs/HBsAb

ferrocene with the electrode surface. Interestingly, after the immunosensor was incubated with HBsAg solution, a further decrease of the redox peak currents was achieved (Fig. 3f), again indicating the formed immunocomplex might further hinder the electron-transfer pathway of the covalently bounded Fc [19, 41]. Moreover, the peak currents of the redox couple of Fc^{+}/Fc decreased with the increment of HBsAg concentration in the sample solution, which was depended on the degree of the antigen–antibody interaction. In addition, the CVs of the immonosensor after being incubated with HBsAg were extremely stable during continuous potential cycling between 0.2 and 0.65 V for 1 h. These results indicated that the constructed PAA-Fc/Au NPs/HBsAb biofilm could efficiently prevent HBsAb from leakage and retain its high bioactivity.

It is well known that EIS is an excellent technique for investigating the interface properties of surface-modified

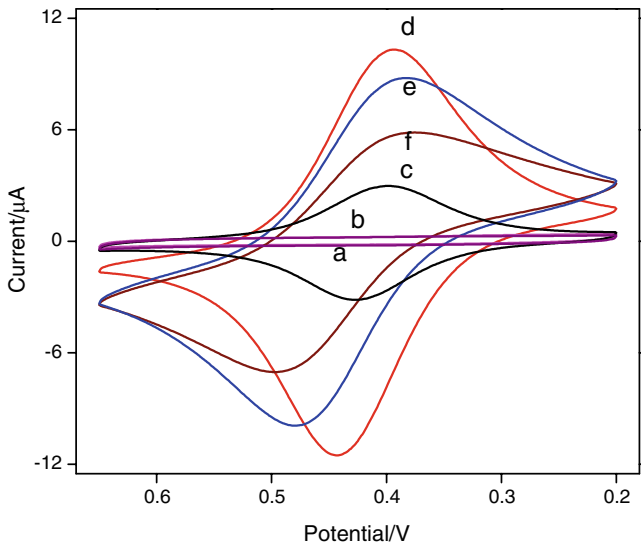

Fig. 3 CVs of different modified electrodes in pH 5.5 acetate buffer containing 0.1 M KCl at a scan rate of 50 mV s^{-1}. **a** bare GCE, **b** PAA, **c** PAA-Fc, **d** PAA-Fc/Au NPs, **e** PAA-Fc/Au NPs/HBsAb modified electrodes, and **f** the modified electrode (**e**) incubated with 50 ng mL^{-1} HBsAg

electrodes. A typical impedance spectrum (presented in the form of the Nyquist plot) exhibits a semicircle near the origin at higher frequencies corresponding to the electron-transfer-limited process and a linear tail at lower frequency range representing the diffusion-limited process. The electron-transfer resistance, R_{et}, is the most directive and sensitive parameter that responds to changes on the electrode interface, as represented by the diameter of the semicircle in the Nyquist plot. Figure 4 shows the impedance spectra corresponding to the stepwise modification processes. The data can be fitted with a modified Randles equivalent circuit (inset in Fig. 4). The bare GCE exhibited an almost straight line in the Nyquist plot of impedance spectroscopy, implying the characteristic of a diffusional limiting step of the electrochemical process (Fig. 4a). After deposition of a PAA layer, the value of R_{et} increased to 158 Ω (Fig. 4b), indicating the successful formation of PAA film obstructed the electron-transfer of the electrochemical probe. When Fc was covalently bounded in PAA, the R_{et} of the resultant PAA-Fc film decreased to 119 Ω (Fig. 4c), which manifested that the formed PAA-Fc membrane benefited the electron-transfer of the electrochemical probe. After Au NPs were assembled on PAA-Fc film, the R_{et} of the resultant PAA-Fc/Au NPs film surprisingly decreased to 63 Ω (Fig. 4d), this may be ascribed to that Au NPs acted as high electron relay for shuttling electron between the electrochemical probe and the electrode. When HBsAb was immobilized, the R_{et} increased dramatically to 323 Ω (Fig. 4e), and the R_{et} increased again (373 Ω) after the electrode was blocked with BSA (Fig. 4f). Especially, after HBsAg molecules were coupled onto the PAA-Fc/Au NPs/HBsAb modified electrode, a remarkable increase of interfacial resistance, 456 Ω, was obtained (Fig. 4g). The reason is that the formation of immunocomplex layer on the electrode acted as the electron communication and mass-transfer blocking layer, further insulating the conductive support and hindering the access of redox probe toward the electrode surface significantly, thus, a further increase in R_{et} was observed [42, 43]. The EIS change of the modified process indicated

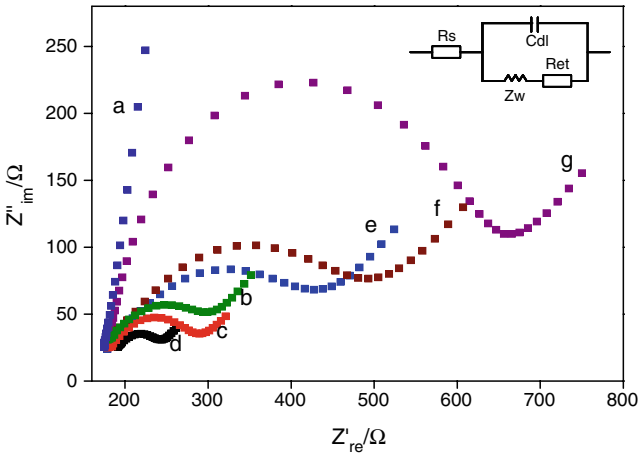

Fig. 4 Nyquist plots of the different electrodes in a acetate buffer (0.1 M, pH 5.5) solution containing 0.1 M KCl and 2.5 mM $Fe(CN)_6^{3-/4-}$: **a** bare GCE, **b** PAA, **c** PAA-Fc, **d** PAA-Fc/Au NPs, **e** PAA-Fc/Au NPs/HBsAb, **f** PAA-Fc/Au NPs/HBsAb/BSA, and **g** PAA-Fc/Au NPs/HBsAb/HBsAg electrodes. Inset: equivalent electrical circuit diagram of the electrochemical interface used to fit the impedance spectra. R_s, Z_w, R_{et}, and C_{dl} represent the solution resistance, the Warburg diffusion resistance, the electron-transfer resistance, and the double layer capacitance, respectively

that the HBsAb was immobilized on the PAA-Fc/Au NPs film electrode surface firmly and retained high bioactivity, which was in good agreement with the CV results.

Optimization of experimental conditions

The factors such as incubation time and incubation temperature of detection solution, influencing the performances of the immunosensor were investigated. Because it takes time for the antigens in the incubation solution to combine with the antibodies at the surface of the immunosensor, the fabricated immunosensor was incubated for 0–20 min in 50 ng mL^{-1} HBsAg solution. It was found that the amperometric signal decreased with the incubation time up to 10 min and then leveled off slowly (see Fig. S1a, ESM), manifesting that the antigen molecules in the incubation solution were substantially captured by the immobilized antibody molecules. A longer incubation time did not improve the response. Thus, 10 min was chosen as the optimal incubation time for the antigen–antibody interaction. The pH value of the detection solution was also an important parameter, and unsuitable pH may cause protein denaturalization or immunosensor unstable [44]. The effect of incubation temperature on the current value for the antibody–antigen immunoreaction was examined in a temperature range of 15–50 °C. As shown in Fig. S1b, the current response of the immunosensor after incubation with HBsAg decreased with increasing temperature up to 35 °C, indicating that an increase of temperature had a favorable effect on the immunoreaction using constant concentration of HBsAg. However, the amperometric response increased quickly as the temperatures over 40 °C, implying the antibody/antigen complex on the electrode could be damaged at a higher temperature. Therefore, 35 °C was selected for this study.

Performance of the immunosensor

Under optimized conditions, differential pulse voltammetry (DPV) was employed to investigate the immunoreaction between the immobilized HBsAb and HBsAg in the sample. The quantitative measurement was determined from 0.2 to 0.68 V (vs Ag/AgCl) with a pulse amplitude of 50 mV and a pulse width of 50 ms in 0.1 M pH 5.5 acetate buffer solution. As can be seen from Fig. 5, the DPV peak currents show a decrease with the increment of HBsAg concentration. It can be understood that more antigen molecules could bind to the immobilized antibodies at higher concentrations of antigens, and the antigen–antibody complex acted as an inert kinetic barrier for the electron-transfer of the Fc mediator. As a result, the amperometric response decreased with increase of the HBsAg concentration [45]. As presented in the inset of Fig. 5, the decrease of DPV peak current is proportional to HBsAg concentration in the range of 0.1–150.0 ng mL^{-1} with a detection limit of 0.04 ng mL^{-1} at the signal-to-noise ratio of 3, which was less than those reported 10 ng mL^{-1} [46], 3.89 ng mL^{-1} [47], 2.3 ng mL^{-1} [48], 0.7 ng mL^{-1} [49], and 0.42 ng mL^{-1} [50]. According to the linear equation, the HBsAg concentration could be detected quantitatively.

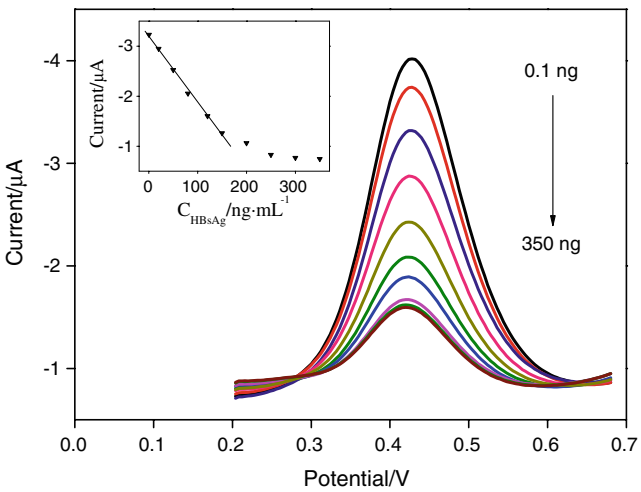

Fig. 5 DPV curves of the immunosensor after incubating with various concentrations of HBsAg in 0.1 M pH 5.5 acetate buffer solution: 0.1, 20, 50, 80, 120, 150, 200, 250, 300, and 350 ng mL^{-1} (from *top* to *bottom*). Inset: Calibration curve of the immonosensor for HBsAg determination

Reproducibility, stability and selectivity of the immunosensor

The reproducibility of the resulted immunosensor was investigated at HBsAg concentration of 50 ng mL^{-1}. Seven immunosensors, made independently, showed an acceptable relative standard deviation (RSD) of 3.6%, suggested that the electrode-to-electrode reproducibility of the fabrication protocol was satisfactory. The storage stability was tested over a 30 days period when the sensor was stored at 4 °C. It was measured intermittently (every 3~5 days), no obvious change of the amperometric response was found over this period, indicating the effective retention of the activity of the immobilized HBsAb. A long storage period of 30 days also indicated that the PAA-Fc/Au NPs composite structure was very efficient for retaining the bioactivity of the immobilized HBsAb and preventing the HBsAb from leakage. Nonspecific adsorption is the major problem in label-free immunosensing. Possible interfering substances were used to evaluate the selectivity of the present immunosensor. The immunosensors were incubated with 50 ng mL^{-1} HBsAg, respectively containing the same concentration of CEA, AFP, BSA, l-cysteine, or l-glutamic acid, no remarkable difference in DPV peak currents for these systems was observed as compared to the pure HBsAg system, demonstrating a good selectivity of the immunoassay.

Application of the immunosensors

In order to demonstrate the use of the fabricated immunosensor for the determination of the HBsAg in human serum, six serum samples from the hospital affiliated to our university were examined by the developed electrochemical immunosensor. 0.5 mL serum sample was diluted to 2 mL with PBS, and then the as-prepared immunosensor was incubated in the above solution at 35 °C for 10 min. After a washing step with acetate buffer solution, the current measurement was carried out in pH 5.5 acetate buffer solution containing 0.1 M $KClO_4$. The results were compared with those obtained by ELISA (see Table S1, ESM). The relative deviations between two methods were in the range of −5.76 to +6.12%, which indicated the two methods were in acceptable agreement. Hence, the developed immunoassay might provide a feasible alternative tool for determining the HBsAg in human serum in a clinical laboratory.

Conclusion

In this paper, we report on the development of a novel approach for fabrication of a label-free amperometric immunosensor based on immobilization of antibody molecules on biocompatible redox-active PAA-Fc/Au NPs composite film. The formation of PAA-Fc composite not only avoided the leakage of Fc from the matrix, but also retained its electrochemical activity. Moreover, Au NPs with larger specific interface areas, desirable biocomapatibility, and a high surface free energy could absorb more antibodies without loss of their biological activities. The fabrication is convenient and cost-effective, which is valuable for clinical immunoassays and could be extended readily to the preparation of other amperometric immunosensors.

Acknowledgments This work was supported by grants from the National Natural Science Foundation of China (20865003, 20805023, 21065006), the Jiangxi Province Natural Science Foundation (2007JZH2644), and the Program for Young Scientists of Jiangxi Province (2008222).

References

1. Gitlin N (1997) Hepatitis B: diagnosis, prevention, and treatment. Clin Chem 43:1500–1506
2. Satoh K, Iwata-Takakura A, Yoshikawa A, Gotanda Y, Tanaka T, Yamaguchi T, Mizoguchi H (2008) A new method of concentrating hepatitis B virus (HBV) DNA and HBV surface antigen: an application of the method to the detection of occult HBV infection. Vox Sang 95:174–180
3. Lee HS, Han CJ, Kim CY (1993) Predominant etiologic association of hepatitis C virus with hepatocellular carcinoma compared with hepatitis B virus in elderly patients in a hepatitis B-endemic area. Cancer 72:2564–2567
4. Zhang S, Zou J, Yu F (2008) Investigation of voltammetric enzyme-linked immunoassay based on a new system of HAP-H_2O_2-HRP. Talanta 76:122–127
5. Siitari H, Hemmila I, Soini E, Lovgren T, Koistinen V (1983) Detection of hepatitis B surface antigen using time-resolved fluoroimmunoassay. Nature 301:258–260
6. Chen D, Kaplan LA (2006) Performance of a new-generation chemiluminescent assay for hepatitis B surface antigen. Clin Chem 52:1592–1598
7. Wu J, Fu Z, Yan F, Ju H (2007) Biomedical and clinical applications of immunoassays and immunosensors for tumor markers. TrAC Trends Anal Chem 26:679–688
8. Liu ZY, Yuan R, Chai YQ, Zhuo Y, Hong CL, Yang X (2008) Highly sensitive, reagentless amperometric immunosensor based on a novel redox-active organic-inorganic composite film. Sens Actuators B 134:625–631
9. Aguilar ZP, Vandaveer WR, Fritsch I (2002) Self-contained microelectrochemical immunoassay for small volumes using mouse IgG as a model system. Anal Chem 74:3321–3329
10. Yuan R, Zhang L, Li Q, Chai Y, Cao S (2005) A label-free amperometric immunosenor based on multi-layer assembly of polymerized o-phenylenediamine and gold nanoparticles for determination of Japanese B encephalitis vaccine. Anal Chim Acta 531:1–5
11. Berggren C, Johansson G (1997) Capacitance measurements of antibody-antigen interactions in a flow system. Anal Chem 69:3651–3657
12. Yeo J, Park JY, Bae WJ, Lee YS, Kim BH, Cho Y, Park SM (2009) Label-free electrochemical detection of the p53 core

domain protein on its antibody immobilized electrode. Anal Chem 81:4770–4777
13. Chua JH, Chee RE, Agarwal A, Wong SM, Zhang GJ (2009) Label-free electrical detection of cardiac biomarker with complementary metal-oxide semiconductor-compatible silicon nanowire sensor arrays. Anal Chem 81:6266–6271
14. Zhang J, Lei JP, Xu CL, Ding L, Ju HX (2010) Carbon nanohorn sensitized electrochemical immunosensor for rapid detection of microcystin-LR. Anal Chem 82:1117–1122
15. Zhao G, Zhan X (2010) Facile preparation of disposable immunosensor for Shigella flexneri based on multi-wall carbon nanotubes/chitosan composite. Electrochim Acta 55:2466–2471
16. Santandreu M, Alegret S, Fàbregas E (1999) Determination of [beta]-HCG using amperometric immunosensors based on a conducting immunocomposite. Anal Chim Acta 396:181–188
17. Huang KJ, Sun JY, Xu CX, Niu DJ, Xie WZ (2010) A disposable immunosensor based on gold colloid modified chitosan nanoparticles-entrapped carbon paste electrode. Microchim Acta 168:51–58
18. Zhang LY, Liu Y, Chen T (2009) Label-free amperometric immunosensor based on antibody immobilized on a positively charged gold nanoparticle/L-cysteine-modified gold electrode. Microchim Acta 164:161–166
19. Li N, Yuan R, Chai Y, Chen S, An H, Li W (2007) New antibody immobilization strategy based on gold nanoparticles and Azure I/multi-walled carbon nanotube composite membranes for an amperometric enzyme immunosensor. J Phys Chem C 111:8443–8450
20. Yuan Y, Yuan R, Chai Y, Zhuo Y, Shi Y, He X, Miao X (2007) A reagentless amperometric immunosensor for alpha-fetoprotein based on gold nanoparticles/TiO_2 colloids/prussian blue modified platinum electrode. Electroanalysis 19:1402–1410
21. Lv P, Min LG, Yuan R, Chai YQ, Chen SH (2010) A novel immunosensor for carcinoembryonic antigen based on poly (diallyldimethylammonium chloride) protected prussian blue nanoparticles and double-layer nanometer-sized gold particles. Microchim Acta 171:297–304
22. Das J, Jo K, Lee JW, Yang H (2007) Electrochemical immunosensor using p-aminophenol redox cycling by hydrazine combined with a low background current. Anal Chem 79:2790–2796
23. Tripathi VS, Kandimalla VB, Ju HX (2006) Amperometric biosensor for hydrogen peroxide based on ferrocene-bovine serum albumin and multiwall carbon nanotube modified ormosil composite. Biosens Bioelectron 21:1529–1535
24. Qiu JD, Wang R, Liang RP, Xia XH (2009) Electrochemically deposited nanocomposite film of CS-Fc/Au NPs/GOx for glucose biosensor application. Biosens Bioelectron 24:2920–2925
25. Liu D, Liu H, Hu N (2010) pH-controllable bioelectrocatalysis of glucose by glucose oxidase loaded in weak polyelectrolyte layer-by-layer films with ferrocene derivative as mediator. Electrochim Acta 55:6426–6432
26. Zhang SX, Fu YQ, Sun CQ (2003) Fabrication of poly(allylamine)ferrocene monolayer based on electrostatic interaction and its electrocatalytic oxidation of ascorbic acid. Electroanalysis 15:739–746
27. Deng L, Liu Y, Yang G, Shang L, Wen D, Wang F, Xu Z, Dong S (2007) Molecular "wiring" glucose oxidase in supramolecular architecture. Biomacromolecules 8:2063–2071
28. Ho JA, Chang HC, Shih NY, Wu LC, Chang YF, Chen CC, Chou C (2010) Diagnostic detection of human lung cancer-associated antigen using a gold nanoparticle-based electrochemical immunosensor. Anal Chem 82:5944–5950
29. Yuan YR, Yuan R, Chai YQ, Zhuo Y, Miao XM (2009) Electrochemical amperometric immunoassay for carcinoembryonic antigen based on bi-layer nano-Au and nickel hexacyanoferrates nanoparticles modified glassy carbon electrode. J Electroanal Chem 626:6–13
30. Cui RJ, Huang HP, Yin ZZ, Gao D, Zhu JJ (2008) Horseradish peroxidase-functionalized gold nanoparticle label for amplified immunoanalysis based on gold nanoparticles/carbon nanotubes hybrids modified biosensor. Biosens Bioelectron 23:1666–1673
31. Wang F, Hu SS (2009) Electrochemical sensors based on metal and semiconductor nanoparticles. Microchim Acta 165:1–22
32. Hodak J, Etchenique R, Calvo EJ, Singhal K, Bartlett PN (1997) Layer-by-layer self-assembly of glucose oxidase with a poly (allylamine)ferrocene redox mediator. Langmuir 13:2708–2716
33. Qiu JD, Peng HZ, Liang RP, Li J, Xia XH (2007) Synthesis, characterization, and immobilization of prussian blue-modified Au nanoparticles: application to electrocatalytic reduction of H_2O_2. Langmuir 23:2133–2137
34. Siebrands T, Giersig M, Mulvaney P, Fischer CH (1993) Steric exclusion chromatography of nanometer-sized gold particles. Langmuir 9:2297–2300
35. Hu MH, Yamaguchi Y, Okubo T (2005) Self-assembly of water-dispersed gold nanoparticles stabilized by a thiolated glycol derivative. J Nanopart Res 7:187–193
36. Zhou YL, Li YZ (2004) Studies of interaction between poly (allylamine hydrochloride) and double helix DNA by spectral methods. Biophys Chem 107:273–281
37. Park MK, Deng SX, Advincula RC (2004) pH-sensitive bipolar ion-permselective ultrathin films. J Am Chem Soc 126:13723–13731
38. Burke SE, Barrett CJ (2004) pH-dependent loading and release behavior of small hydrophilic molecules in weak polyelectrolyte multilayer films. Macromolecules 37:5375–5384
39. Huang HZ, Yang XR (2003) Chitosan mediated assembly of gold nanoparticles multilayer. Colloids Surf A 226:77–86
40. Chen J, Yan F, Du D, Wu J, Ju HX (2006) Electrochemical immunoassay of human chorionic gonadotrophin based on its immobilization in gold nanoparticles-chitosan membrane. Electroanalysis 18:670–676
41. Wu Y, Zheng JW, Li Z, Zhao YR, Zhang Y (2009) A novel reagentless amperometric immunosensor based on gold nanoparticles/TMB/Nafion-modified electrode. Biosens Bioelectron 24:1389–1393
42. Zhuo Y, Yuan R, Chai YQ, Tang DP, Zhang Y, Wang N, Li XL, Zhu Q (2005) A reagentless amperometric immunosensor based on gold nanoparticles/thionine/Nafion-membrane-modified gold electrode for determination of alpha-1-fetoprotein. Electrochem Commun 7:355–360
43. Zhuo Y, Yuan PX, Yuan R, Chai YQ, Hong CL (2008) Nanostructured conductive material containing ferrocenyl for reagentless amperometric immunosensors. Biomaterials 29:1501–1508
44. Zhou L, Yuan R, Chai YQ (2007) On-off PVC membrane based potentiometric immunosensor for label-free detection of alpha-fetoprotein. Electroanalysis 19:1131–1138
45. Qiu JD, Liang RP, Wang R, Fan LX, Chen YW, Xia XH (2009) A label-free amperometric immunosensor based on biocompatible conductive redox chitosan-ferrocene/gold nanoparticles matrix. Biosens Bioelectron 25:852–857
46. Lee HJ, Namkoong K, Cho EC, Ko C, Park JC, Lee SS (2009) Surface acoustic wave immunosensor for real-time detection of hepatitis B surface antibodies in whole blood samples. Biosens Bioelectron 24:3120–3125
47. Liang RP, Peng HZ, Qiu JD (2008) Fabrication, characterization, and application of potentiometric immunosensor based on biocompatible

and controllable three-dimensional porous chitosan membranes. J Colloid Interface Sci 320:125–131
48. Yuan R, Tang DP, Chai YQ, Zhong X, Liu Y, Dai JY (2004) Ultrasensitive potentiometric immunosensor based on SA and OCA techniques for immobilization of HBsAb with colloidal Au and polyvinyl butyral as matrixes. Langmuir 20:7240–7245
49. Hanaee H, Ghourchian H, Ziaee AA (2007) Nanoparticle-based electrochemical detection of hepatitis B virus using stripping chronopotentiometry. Anal Biochem 370:195–200
50. Tang DY, Xia BY (2008) Electrochemical immune bioassay for the antigen–antibody interaction based on $Fe(CN)_6^{4-/3-}$ and $AuCl_4^-$ ions-derivated biomimetic interface. Ionics 14:329–334